**Preprints of the 21st IFAC World Congress (Virtual)**
**Berlin, Germany, July 12-17, 2020**

# Tip Tracking Control of a Linear-Motor-Driven Flexible Manipulator with Controllable Damping ⋆

**Xiaocong Zhu** * **Xinda Shen** * **Linyuan Wang** * **Jian Cao** **

* *State Key Laboratory of Fluid Power and Mechatronic Systems, Zhejiang University, Hangzhou, 310027, China (e-mail: zhuxiaoc@zju.edu.cn, xindashen@zju.edu.cn, wang-linyuan@qq.com).*
** *School of Mechanical Engineering, Hefei University of Technology, Hefei,China (e-mail: caojianjiaowang@sina.com)*

**Abstract:** In this paper, a linear-motor-driven flexible robotic manipulator with controllable damping is presented. The dynamic model of the flexible manipulator with magnetorheological(MR) dampers is established through analyzing the force constraint of controllable MR damping and the rigid-flexible coupling dynamics of entire system via Lagrange method and assumed mode method. A controller for the flexible manipulator with MR dampers is developed to realize the dual targets of vibration suppression and accurate tip tracking for the flexible manipulator. The controller integrated output redefine adaptive robust control based on the system dynamics with damping control law according to motion state of the flexible system. Simulation results verifies the effectiveness of the proposed control method.

*Keywords:* Flexible manipulator, Magnetorheological damper, Vibration suppression, Adaptive robust control, Tip tracking, Controllable damping

## 1. INTRODUCTION

The flexible manipulator has been used in many fields owning to its superior advantages compare to the rigid manipulator, such as light structure weight with less material, low energy consumption with small driving force needed etc.(Lochan et al. (2016)). Unfortunately, there may be severe link vibration occurred during the process of movement due to its flexible structure. Therefore, it is necessary to consider attenuation of vibration when designing the positioning or trajectory tracking control of the flexible manipulator.

Up to now, various control algorithms have been developed for the tip tracking control of the flexible manipulator with one controllable actuator placed at the base (i.e., non-allocated placement of one actuator and sensors). In general, the control design can be classified into the three categories: (1)Control design without considering system dynamic model. Specifically, Ouyang et al. (2017) proposed a method using reinforcement learning and neural network to suppress the vibration of the rotating flexible manipulator. (2)Control design based on system dynamic model. Specifically, Liao et al. (2016) proposed an adaptive robust control (ARC) algorithm using output redifination for the linear-motor-driven flexible manipulator. (3) Control design with input shaping technique. Specifically, Zhang et al. (2015) utilized input shaping to suppress the vibration generated by the motion of flexible manipulator.

It is noticed that there is dual objects for the motion control of the flexible manipulator, i.e., precision tip tracking control and good vibration suppression. The available tip tracking performance of the flexible system is prone to be limited by the vibration of the link. As analyzed for the non-allocated flexible system, the effect of vibration suppression is significantly influenced by the system damping. Hence, it is useful to add another actuator with controllable damping and implement damping control to realize quick vibration attenuation of the system. The controllable damping used in flexible systems includes piezoelectric actuator (Dadfarnia et al. (2004)), electrorheological elastomer (ERE) (Li et al. (2015)), magnetorheological elastomer (MRE)(Lara-Prieto et al. (2009)), memory alloy (McCormick et al. (2006)) etc. Specially, Kumar et al. (2014) compared the suppression effect of mounting piezoelectric actuator on the root, middle and tip of the cantilever respectively, and concluded that mounting piezoelectric actuator at the root of the cantilever had the best effectiveness. Thereinto, Magnetorheological (MR) dampers, which can realize adjustable damping when applied different current to control the magnetic field, have been widely used in various fields (Sun et al. (2015)). Considering convenient damping control of MR dampers, a linear-motor-driven flexible manipulator with controllable MR dampers is presented to further decrease the vibration during tip tracking control of the flexible manipulator.

This paper is organized as follows. In Section 2, the schematics of the flexible manipulator with controllable

⋆ This work is supported by National Natural Science Foundation of China (No.51675471 and No.51375432), and Science Fund for Creative Research Groups of National Natural Science Foundation of China (No.51821093), and also supported by the Fundamental Research Funds for the Central Universities (2019QNA4002).
⋆⋆Address all correspondence to Jian Cao.

MR damping is introduced, and the dynamic model of the flexible system is analyzed. In Section 3, the tip tracking control design for the flexible system with controllable damping is synthesized. In Section 4, the performance testing of vibration suppression and tip trajectory tracking for the flexible system are conducted. In Section 5, conclusions and further work are considered.

## 2. SYSTEM MODELING

### 2.1 Flexible manipulator with controllable damping

The test-rig of the linear-motor-driven flexible manipulator with controllable damping is shown in Fig. 1. As shown, the single-link flexible beam is driven by a linear motor and two MR dampers mounted at the base end of the beam. The deflection of the flexible link is detected by the piezoelectric sensor mounted on the root of the flexible link and the tip deflection signal is further validated by the laser sensor. A linear encoder, which is connected with the linear motor, is used to measure the position of the linear motor. The controllable damping is realized by adjusting the applied current to the MR damper via amplifier. The real-time measured signals are received through the AI and DI parts of the control unit, and the applied voltages for MR dampers and the linear motor are output to the AO parts of the control unit after calculation via certain control algorithm.

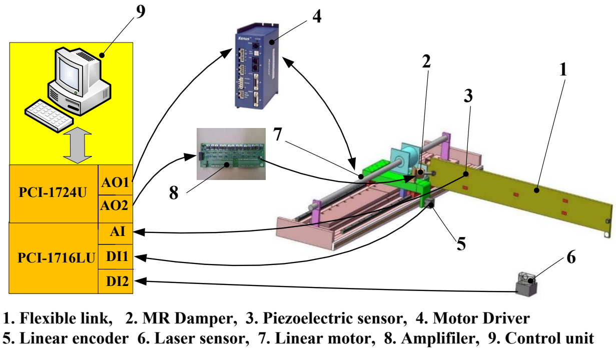


Fig. 1. Test-rig design of the linear-motor-driven flexible manipulator with MR dampers

### 2.2 Force constraint of controllable damping

The flexible link with controllable damping can be equivalent to the cantilever when the linear motor is not moving. The schematics of the cantilever with MR dampers is shown in Fig. 2.

The output force of the MR damper is given by Bingham model (Spencer Jr et al. (1997))

$$F_d = b_c\dot{q} + A_\tau(I)sign(\dot{q}) \tag{1}$$

where, $q$ is the rod displacement of the MR damper, $\dot{q}$ is the rod speed of the MR damper, $b_c$ is the viscous friction coefficient, and $A_\tau(I)$ is the controllable damping force dependent on the applied current $I$.

The vibration of a homogeneous beam with the uniform load can be described as Wang (2019)

$$\rho A_b \sum_{i=1}^{n} \nu_i^2 \varphi_i(x) q_i(t) + \rho A_b \sum_{i=1}^{n} \varphi_i(x)\ddot{q}_i(t) = f(x,t) \tag{2}$$

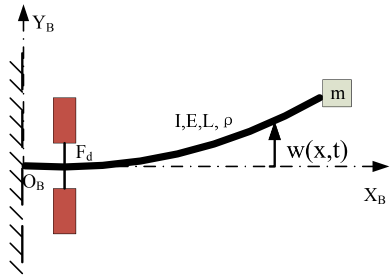


Fig. 2. Schematics of a cantilever with uniformed load

where, $\rho$ is density of the beam, $A_b$ is the cross-sectional area of the beam, $\nu_i$ is the natural frequency of the vibration mode, $\varphi_j(x)$ is the modal function, $q_i(t)$ is the generalized coordinates, $f(x,t)$ is the applied uniform force on the beam.

The modal orthogonalization is satisfied.

$$\int_0^L \rho A_b \varphi_i(x)\varphi_j(x)dx + m\varphi_i(L)\varphi_j(L) = \delta_{i,j} \tag{3}$$

where, $\delta_{ij}$ is Kronecker delta, $m$ is the load mass at the tip end of the beam.

If the load mass at the tip end of the beam is zero, one obtains

$$\int_0^L \rho A_b \varphi_i(x)\varphi_j(x)dx = \delta_{ij} \tag{4}$$

Multiply both sides of (4) with $\nu_i$, one obtains

$$\nu_i^2 \int_0^L \rho A_b \varphi_i(x)\varphi_j(x)dx = \nu_i^2\delta_{ij} \tag{5}$$

Multiply both sides of (2) with $\varphi_j(x)$ and integrate two sides of the equation, one obtains

$$\rho A_b\Big(\sum_{i=1}^{n}\int_0^L \nu_i^2\varphi_i(x)\varphi_j(x)q_i(t) + \sum_{i=1}^{n}\int_0^L \varphi_i(x)\varphi_j(x)\ddot{q}_i(t)\Big) = \int_0^L \varphi_j(x)f(x,t)dx \tag{6}$$

Substitute (4) and (5) into (6), then one obtains

$$\sum_{i=1}^{n}\delta_{ij}\nu_i^2 q_i(t) + \sum_{i=1}^{n}\delta_{ij}\ddot{q}_i(t) = \int_0^L \varphi_j(x)f(x,t)dx \tag{7}$$

When $i = j$, we have

$$\ddot{q}_i + \nu_i^2 q_i = \int_0^L \varphi_i(x)f(x,t)dx \tag{8}$$

If considering the structure damping of the flexible beam, the dynamic equation of the cantilever with controllable MR damping is given by

$$\ddot{q}_i + d_i\nu_i\dot{q}_i + \nu_i^2 q_i = \int_0^L \varphi_i(x)f(x,t)dx \tag{9}$$

The left side of (9) can be regarded as the applied torque of the flexible beam, which is dependent on the damping force exerted by MR dampers concentrates on one section at the root of the cantilever between the position from $x_1$ to $x_2$. the force constraint of controllable damping by

MR dampers on the cantilever (i.e., the applied torque) is written as follow through substituting (1) into it.

$$\tau_{q_i} = \int_0^L \varphi_i(x) f(x,t)dx = \int_{x_1}^{x_2} \varphi_i(x) F_d dx = k_{dpi} * [b_c \dot{q}_i + A_\tau(I) sign(\dot{q}_i)] \tag{10}$$

where, $k_{dpi} = \int_{x_1}^{x_2} \varphi_i(x)dx$.

*2.3 Modeling of the entire flexible system*

Next, the dynamic model of the flexible manipulator with controllable MR damping is developed by integrating Lagrange method with the constraint force of MR dampers. The schematics of the linear-motor-driven flexible manipulator with controllable MR damping is shown in Fig. 3, the tip position of the beam is given by

$$y_t(x,t) = p(t) + w(x,t) = p(t) + \sum_{i=1}^{n} \varphi_i(x) q_i(t) \tag{11}$$

where, $p(t)$ is the position of the linear motor, and $w(x,t)$ is the tip deflection of the flexible link.

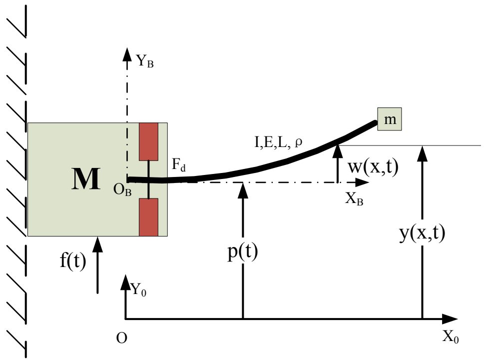


Fig. 3. Schematics of the linear-motor-driven flexible manipulator with controllable damping system

The kinetic and potential energies of the flexible link based on controllable damping are given by

$$E_k = \frac{1}{2} M \dot{p}^2(t) + \frac{1}{2}\rho A_b \int_0^L \dot{y}^2(x,t)dx + \frac{1}{2} m \dot{y}^2(L,t) \tag{12}$$

$$E_p = \frac{1}{2} EI \int_0^L [w''(x,t)]^2 dx \tag{13}$$

where, $M$ is the total mass including the motor and MR dampers.

Lagrange method is employed to describe the dynamics of the system ,i,e,

$$\frac{d}{dt}\left(\frac{\partial \ell}{\partial \dot{Q}}\right) - \frac{\partial \ell}{\partial Q} = F \tag{14}$$

where, $Q = (p, q_1, q_2, ..., q_n)^T$, $\ell = E_k - E_p$, $F = [F_M, \tau_{q_1}, \tau_{q_2}, ..., \tau_{q_n}]^T$, $F_M$ is the motor driving force, $\tau_{q_i}$ is the output force of the MR damper given by (10).

Through substituting (12) and (13) into (14), one obtains

$$\frac{d}{dt}\left(\frac{\partial \ell}{\partial \dot{p}}\right) - \frac{\partial \ell}{\partial p} = F_M \tag{15}$$

$$\frac{d}{dt}\left(\frac{\partial \ell}{\partial \dot{q}_i}\right) - \frac{\partial \ell}{\partial q_i} = \tau_{q_i} \tag{16}$$

where,

$$\frac{d}{dt}\left(\frac{\partial \ell}{\partial \dot{p}}\right) = (M + \rho A_b L + m)\ddot{p} + \sum_{i=1}^{n} \Big(\rho A_b \int_0^L \varphi_i(x)dx + m\varphi_i(L)\Big)\ddot{q}_i \tag{17}$$

$$\frac{\partial \ell}{\partial p} = 0 \tag{18}$$

$$\frac{d}{dt}\left(\frac{\partial \ell}{\partial \dot{q}_i}\right) = \Big(\rho A_b \int_0^L \varphi_i(x)dx + m\varphi_i(L)\Big)\ddot{p} + \Big(\rho A_b \int_0^L \varphi_i(x)^2 dx + m\varphi_i^2(L)\Big)\ddot{q} \tag{19}$$

$$\frac{\partial \ell}{\partial q_i} = -EI \int_0^L \left(\frac{\partial^2 \varphi_i(x)}{\partial x^2}\right)^2 dx q_i \tag{20}$$

According to the modal orthogonalization (Wang (2019)), one obtains,

$$EI \int_0^L \frac{\partial^2 \varphi_i(x)}{\partial x^2} \frac{\partial^2 \varphi_j(x)}{\partial x^2} dx = \nu_i^2 \delta_{i,j} \tag{21}$$

Through simplification of above equations, the dynamic equation of the flexible manipulator with controllable damping can be written as

$$\sum_{i=1}^{n} \Big(\rho A_b \int_0^L \varphi_i(x) dx + m\varphi_i(L)\Big)\ddot{q}_i(t) + (M + m + \rho A_b L)\ddot{p}(t) = F_M \tag{22}$$

$$\Big(\rho A_b \int_0^L \varphi_i(x) dx + m\varphi_i(L)\Big)\ddot{p}(t) + \ddot{q}_i(t) + 2\xi_i \nu_i \dot{q}_i(t) + \nu_i^2 q_i(t) = \tau_{q_i} \tag{23}$$

where, $i = 1, 2, ..., n$. The driving force of the linear motor is given by

$$F_M = k_{mt} u - A_f S_f(\dot{p}) - b_v \dot{p} + \Delta_f \tag{24}$$

where, $S_f(\dot{p}) = sign(\dot{p})$ is the function used to represent Coulumb friction, and $\Delta_f$ is the force disturbance.

Considering the first-order mode of the flexible manipulator, the dynamic equation of the entire flexible system is written as

$$a_0 \ddot{p} + a_1 \ddot{q}_1 = k_{mt} u - A_f sign(\dot{p}) - b_v \dot{p} + \Delta_1 \tag{25a}$$

$$a_1 \ddot{p} + \ddot{q}_1 + d_1 \nu_1 \dot{q}_1 + \nu_1^2 q_1 + \Delta_2 = \tau_{q_1} \tag{25b}$$

$$y_t = p + w(x,t) = p + \sum_{i=1}^{n} \varphi_i(L) q_i \tag{25c}$$

where, $a_0 = M + m + \rho A_b L$, $a_i = \rho A_b \int_0^L \varphi_i(x) dx + m\varphi_i(L)$, $d_1 = 2\xi_1$, $\Delta_1 = \Delta_f - \sum_{i=2}^{n} a_i \ddot{q}_i$, $\Delta_2$ is the modeling error due to MR dampers.

The tip trajectory can be rewritten as

$$y_t = p + L\alpha \tag{26}$$

where, $\alpha$ represents the deflection of the link, and $w(L,t) = L\alpha$,

From (25) and (26), the dynamic model of the entire system with uncertainties can be given by

$$\ddot{p} = \zeta_1 u + \zeta_{13}\tau_{q_1} + \zeta_2 \alpha + \zeta_3 \dot{p} + \zeta_4 \dot{\alpha} + \zeta_9 sign(\dot{p}) + \Delta_p \tag{27a}$$

$$\ddot{\alpha} = \zeta_5 u + \zeta_{14}\tau_{q_1} + \zeta_6 \alpha + \zeta_7 \dot{p} + \zeta_8 \dot{\alpha} + \zeta_{10} sign(\dot{p}) + \Delta_\alpha \tag{27b}$$

where, $\zeta_1 = \frac{1}{\left(a_0 - a_1^2\right)} k_{mt}$, $\zeta_2 = \frac{a_1 \nu_1^2}{b_1\left(a_0 - a_1^2\right)}$, $\zeta_3 = -\frac{1}{\left(a_0 - a_1^2\right)} b_v$, $\zeta_4 = \frac{a_1 d_1 \nu_1}{b_1\left(a_0 - a_1^2\right)}$, $\zeta_5 = \frac{-b_1 a_1}{a_0 - a_1^2} k_{mt}$, $\zeta_6 = -\frac{a_0 \nu_1^2}{a_0 - a_1^2}$, $\zeta_7 = \frac{b_1 a_1}{a_0 - a_1^2} b_v$, $\zeta_8 = -\frac{a_0 d_1 \nu_1}{a_0 - a_1^2}$, $\zeta_9 = -\frac{1}{a_0 - a_1^2} A_f$, $\zeta_{10} = -\frac{a_1 b_1}{a_0 - a_1^2} A_f$, $\Delta_p = \frac{a_1}{a_0 - a_1^2}\Delta_1 - \frac{1}{a_0 - a_1^2}\Delta_2$, $\Delta_\alpha = -\frac{a_0}{a_0 - a_1^2}\frac{\varphi_1(L_l)}{L_l}\Delta_1 + \frac{a_1}{a_0 - a_1^2}\frac{\varphi_1(L_l)}{L_l}\Delta_2$ ,$b_1 = \frac{\varphi_1(L)}{L}$, $\zeta_{13} = -\frac{a_1}{a_0 - a_1^2}$, $\zeta_{14} = \frac{a_0 b_1}{a_0 - a_1^2}$.

## 3. CONTROLLER DESIGN

Next, the tip tracking control design for the flexible manipulator with controllable damping is synthesized with integration of output redefined adaptive robust control for the linear-motor-driven flexible manipulator and the adjustable damping of MR damper. A new output of system considering both the tip position and link vibration is redefined as

$$y = p + \psi\alpha \tag{28}$$

According to (27), the dynamics of redefined output is given by

$$\begin{aligned}\ddot{y} =& \zeta_1 u + \psi\zeta_5 u + (\zeta_{13} + \psi\zeta_{14})\tau_{q_1} + (\zeta_2 + \psi\zeta_6)\alpha + (\zeta_3 \\ &+ \psi\zeta_7)\dot{p} + (\zeta_4 + \psi\zeta_8)\dot{\alpha} + (\zeta_9 + \psi\zeta_{10}) sign(\dot{p}) + \zeta_{11} + \psi\zeta_{12}\end{aligned} \tag{29}$$

The tracking error is given by,

$$e_r = y - y_d \tag{30}$$

where, $y_d$ is the desired tip trajectory.

Design the sliding surface of the tracking error as

$$s_r = \dot{e}_r + k_\lambda e_r = \dot{y} - x_{2eq} \tag{31}$$

$$x_{2eq} \triangleq \dot{y}_d - k_\lambda e_r \tag{32}$$

where $k_\lambda$ is a positive value for the convergence of the sliding surface, $x_{2eq}$ can be regraded as the desired value of $\dot{y}$.

The time derivative of $s_r$ can be written as

$$\dot{s}_r = \ddot{y} - \dot{x}_{2eq} \tag{33}$$

Substituting (29) into (33), one obtains

$$\begin{aligned}\dot{s}_r =& \zeta_1 u + \psi\zeta_5 u + (\zeta_{13} + \psi\zeta_{14})\tau_{q_1} + (\zeta_2 + \psi\zeta_6)\alpha + (\zeta_3 + \psi\zeta_7)\dot{p} \\ &+ (\zeta_4 + \psi\zeta_8)\dot{\alpha} + (\zeta_9 + \psi\zeta_{10}) sign(\dot{p}) + \zeta_{11} + \psi\zeta_{12} - \dot{x}_{2eq}\end{aligned} \tag{34}$$

The equation (34) can be rewritten as

$$\dot{s}_r = K_u u - \dot{x}_{2eq} + \phi_r^T \vartheta_r + \tilde{\Delta} \tag{35}$$

where, $\phi_r = [\alpha, \dot{p}, \dot{\alpha}, sign(\dot{p}), 1]^T$ is the regressor vector, $\vartheta_r = [\zeta_2, \zeta_3, \zeta_4, \zeta_9, d_n]^T$,$K_u = \hat{\zeta}_1$ is the parameter vector to be estimated, $\Delta = (\zeta_{13} + \psi\zeta_{14})\tau_{q_1} + \psi\zeta_6\alpha + \psi\zeta_7\dot{p} + \psi\zeta_8\dot{\alpha} + \psi\zeta_{10} sign(\dot{p}) + \zeta_{11} + \psi\zeta_{12}$ is the lumped disturbance, and let $\Delta = d_n + \tilde{\Delta}$ in which $d_n$ is the slow time-varying term and $\tilde{\Delta}$ is the fast time-varying term or the uncertain nonlinearities.

On one hand, the control input of the linear motor is synthesized to have two parts: the model compensation term $u_{da}$ and the robust feedback term $u_{ds}$:

$$u_d = u_{da} + u_{ds} \tag{36}$$

The model compensation term is designed as

$$u_{da} = \frac{1}{K_u}\left(\dot{x}_{2eq} - \phi_r^T \hat{\vartheta}_r\right) \tag{37}$$

where, $\dot{\hat{\vartheta}}_r = \mathrm{Proj}_{\hat{\vartheta}_r}(\Gamma\sigma)$, $\Gamma$ is a positive matrix, $\sigma$ is the adaptive rate, which is designed as $\sigma = \phi_r s_r$. $\mathrm{Proj}_{\hat{\vartheta}_r}$ is a projection mapping defined as follows, and the details can refer to Lu et al. (2012).

$$\mathrm{Proj}_{\hat{\vartheta}_r} = \begin{cases} 0 & \text{if } \ \hat{\vartheta}_{ri} = \vartheta_{ri\,\max} \ \text{ and } \ \bullet > 0 \\ 0 & \text{if } \ \hat{\vartheta}_{ri} = \vartheta_{ri\,\min} \ \text{ and } \ \bullet < 0 \\ \bullet & \text{otherwise} \end{cases} \tag{38}$$

The robust control consists of the linear feedback term $u_{ds1}$ and the nonlinear feedback term $u_{ds2}$

$$u_{ds} = u_{ds1} + u_{ds2} \tag{39}$$

The linear feedback term is synthesized as

$$u_{ds1} = -\frac{k_r}{K_u} s_r \tag{40}$$

where $k_r$ is the feedback gain.

The nonlinear robust feedback term is chosen to satisfy the following equation.

$$s_r K_u u_{ds2} < 0 \tag{41a}$$

$$s_r \left\{K_u u_{ds2} - \left[\phi_r^T \tilde{\vartheta}_r - \tilde{\Delta}\right]\right\} < \varepsilon_r \tag{41b}$$

where $\varepsilon_r$ is a small positive value.

An example of $u_{ds2}$ can be given by

$$u_{ds2} = -\frac{1}{4\varepsilon_r K_u}\left(||\vartheta_{\mathrm{rmax}} - \vartheta_{\mathrm{rmin}}|| \times ||\phi_r|| + \delta_0\right)^2 s_r \tag{42}$$

where $\delta_0$ is a small positive value.

On the other hand, the control input of the damper $\tau_{q_1}$ is synthesized as a piecewise function as follows.

$$\tau_{q_1} = \begin{cases} k_{dp1} A_\tau(I) sign(\dot{\alpha}) & |\dot{y}_d| < c_{\dot{y}_d} \ and \ |\ddot{y}_d| < c_{\ddot{y}_d} \\ 0 & otherwise. \end{cases} \tag{43}$$

where $c_{\dot{y}_d}$ and $c_{\ddot{y}_d}$ are both set to 0.005.

In summary, the control diagram of the flexible manipulator with controllable damping is shown in Fig. 4.

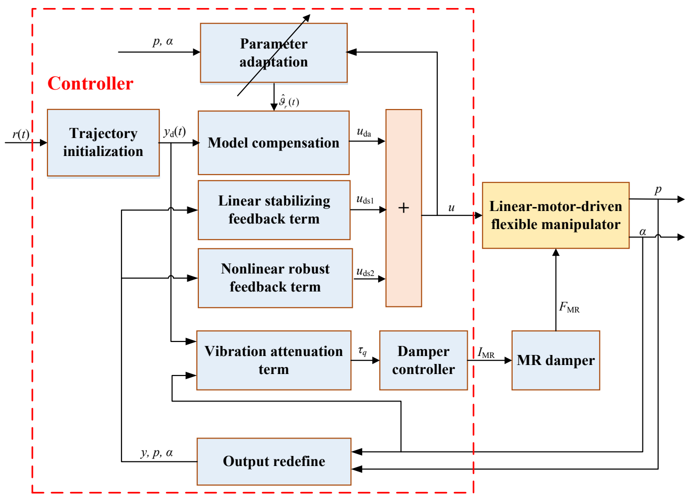


Fig. 4. Control diagram of the flexible manipulator

## 4. SIMULATION RESULTS

Next, the simulation is conducted for the tip tracking control of the flexible manipulator with controllable damping. The physical parameters of the system used in simulation are listed in Tab. 1.

Table 1. Plant parameters of the flexible manipulator

| Name | Unit | Value |
|---|---|---|
| density of link ($\rho$) | $kg/m^3$ | 7850 |
| Young modulus ($E$) | Gpa | 206 |
| rotational inertia of link ($I$) | $kg \cdot m^2$ | 0.0038 |
| length of link ($L$) | m | 0.419 |
| width of link ($W$) | m | 0.001 |
| height of link ($H$) | m | 0.02 |
| end load quality ($m$) | kg | 0 |
| total mass of motor and damper ($M$) | kg | 16 |
| drive force coefficient of motor ($k_{mt}$) | N/V | 45 |
| viscous friction coefficient of motor ($b_v$) | / | 0.7954 |
| Coulomb friction amplitude of motor ($A_f$) | / | 0.2689 |

The tip tracking results of the flexible manipulator with output redefined ARC and adjustable damping control is compared under different working situations. The desired tip trajectory is shown in Fig. 5, which is a point-to-point reciprocating motion and its maximum acceleration is $1.6m/s^2$, maximum speed is $0.8m/s$, and the maximum displacement is $0.4m$. The parameters of the controller are selected as $K_u = 2.8081$, $\Gamma = [0, 0, 0, 0, 50]$, $k_\lambda = 20$, $k_r = 20$. The initial values of the estimated parameters are set to $\hat{\vartheta}_r = [0.3214, -0.0496, 0.0001, 0, 0]^T$, the upper bound and lower bound of the parameters are respectively set to $\vartheta_{max} = [10, 1, 1, 10, 10]^T$,$\vartheta_{min} = [-10, -1, -1, 0, -10]^T$. Two different sets of MR damping (i.e., $k_{dp1}A_\tau(I) = 0$ and $k_{dp1}A_\tau(I) = 0.1$) are utilized for testing. It is indicated that the tip tracking error and the deflection of the flexible manipulator are decreased quickly by applying damping control when the system is nearby its steady-state position (i.e., the absolute value of acceleration of the desired trajectory is less than a constant value and its speed is close to zero), as shown in Fig. 6 and Fig. 7.

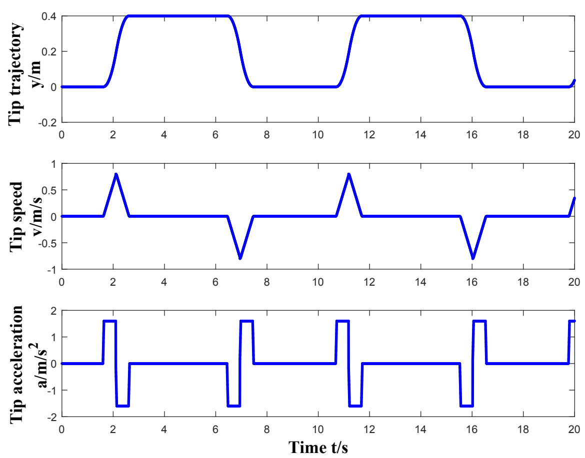


Fig. 5. Slow desired tip trajectory

Next, an increase of the maximum acceleration of $32m/s^2$ and the maximum speed of $1.6m/s$ for the desired tip

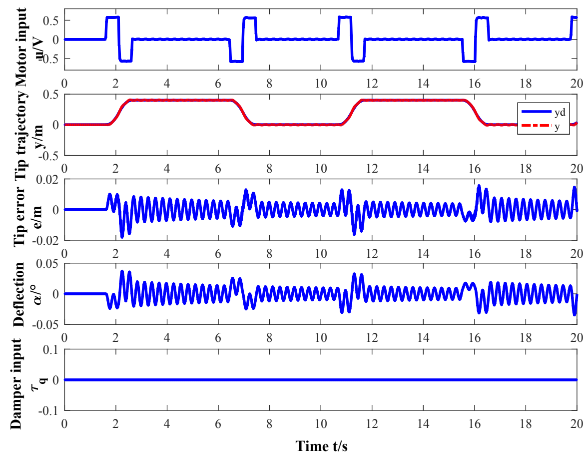


Fig. 6. Slow tip tracking without damping control

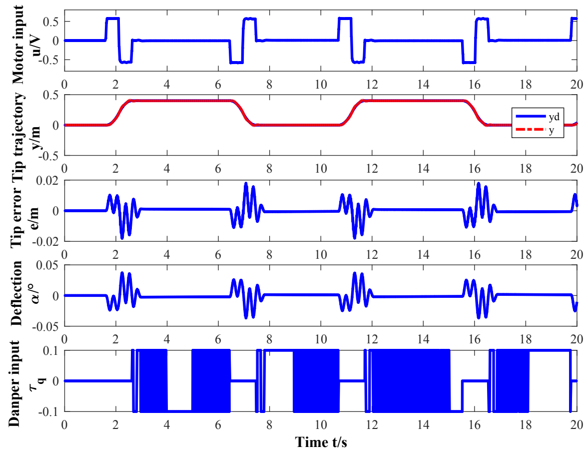


Fig. 7. Slow tip tracking with damping control

trajectory is designed, as shown in Fig. 8. The controller parameters remain unchanged and the tip tracking control with the damper output being $k_{dp1}A_\tau(I) = 0.1$ is shown in Fig. 9. As seen, the tip tracking error and the deflection of the flexible manipulator decreased slowly during the fast tip tracking process. As such, an increase of the damper output $k_{dp1}A_\tau(I) = 0.5$ is used and the simulation result is shown in Fig. 10. As seen, the vibration of the flexible manipulator system is suppressed effectively with the increase of damping. As a result, more stable motion and smaller tip tracking error of the flexible manipulator can be achieved.

## 5. CONCLUSION

This paper focuses on the tip tracking control of the flexible manipulator with controllable damping. The experimental platform design of the linear-motor-driven flexible manipulator with MR dampers is presented. The system dynamics considering the force constraint of MR dampers in addition to conventional dynamics for describing behavior of flexible manipulator is developed. Then the tip tracking controller, which integrated an output redefined adaptive robust control with piece-wise damping control, is synthesized based on the entire dynamics of system. Simulation results indicated the effect of tip vibration suppression and tip tracking control of the flexible manip-

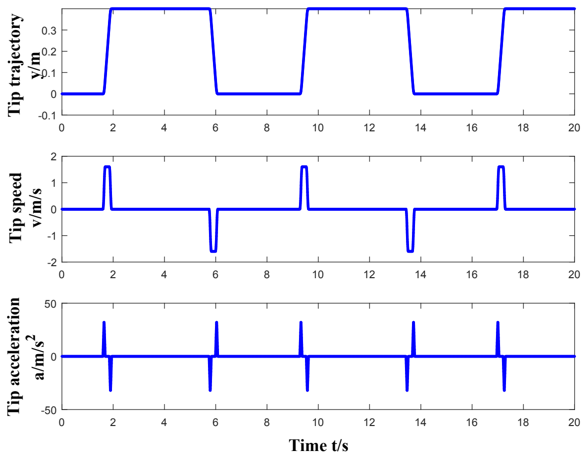


Fig. 8. Fast desired tip trajectory

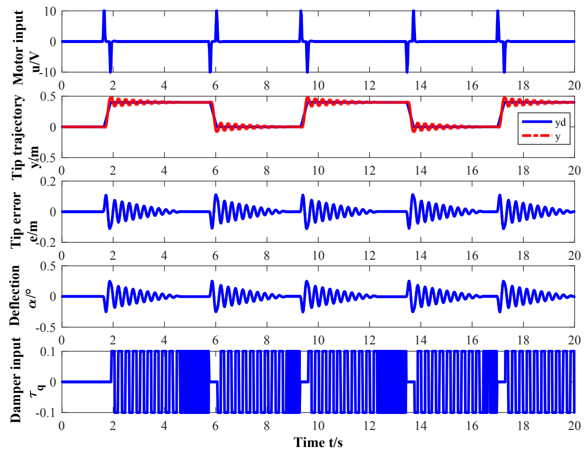


Fig. 9. Fast tip tracking with damping control

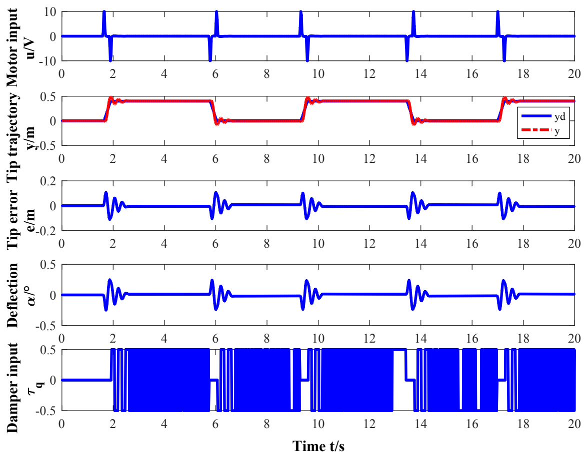


Fig. 10. Fast tip tracking with increased damping control

ulator with the proposed controller. The future research work will include doing the experimental testing of the flexible manipulator to further verify the effect of the proposed method and synthesizing coordinate control law of MR dampers and linear-motor to improve the tip tracking quality subject to various working conditions.

REFERENCES

Dadfarnia, M., Jalili, N., Xian, B., and Dawson, D.M. (2004). A Lyapunov-based piezoelectric controller for flexible cartesian robot manipulators. *Journal of dynamic systems, measurement, and control*, 126(2), 347–358.

Kumar, S., Srivastava, R., and Srivastava, R. (2014). Active vibration control of smart piezo cantilever beam using pid controller. *International Journal of Research in Engineering and Technology*, 3(1), 392–399.

Lara-Prieto, V., Parkin, R., Jackson, M., Silberschmidt, V., and Kesy, Z. (2009). Vibration characteristics of MR cantilever sandwich beams: experimental study. *Smart Materials and structures*, 19(1), 015005.

Li, X., Wei, S., Luo, X., Zhu, J., and Yin, W. (2015). Design and simulation of high-voltage power supply for electron beam precision micro machining equipment. In *2015 2nd International Workshop on Materials Engineering and Computer Sciences*. Atlantis Press.

Liao, J., Li, C., Yao, B., and Zhu, X. (2016). Adaptive robust tip tracking control for single-link flexible beam. In *Proceedings of the ASME 8th Annual Dynamic Systems and Control Conference, 2015, VOL 2.*

Lochan, K., Roy, B., and Subudhi, B. (2016). A review on two-link flexible manipulators. *Annual Reviews in Control*, 42, 346–367.

Lu, L., Chen, Z., Yao, B., and Wang, Q. (2012). A two-loop performance-oriented tip-tracking control of a linear-motor-driven flexible beam system with experiments. *IEEE Transactions on Industrial Electronics*, 60(3), 1011–1022.

McCormick, J., DesRoches, R., Fugazza, D., and Auricchio, F. (2006). Seismic vibration control using superelastic shape memory alloys. *Journal of Engineering Materials and Technology*, 128(3), 294–301.

Ouyang, Y., He, W., and Li, X. (2017). Reinforcement learning control of a single-link flexible robotic manipulator. *IET Control Theory and Applications*, 11(9), 1426–1433.

Spencer Jr, B., Dyke, S., Sain, M., and Carlson, J. (1997). Phenomenological model for magnetorheological dampers. *Journal of engineering mechanics*, 123(3), 230–238.

Sun, S., Yang, J., Li, W., Deng, H., Du, H., and Alici, G. (2015). Development of a novel variable stiffness and damping magnetorheological fluid damper. *Smart Materials and Structures*, 24(8), 085021.

Wang, L. (2019). *Tip Tracking Control of the Flexible Manipulator based on Controllable Damping and Vibration Suppression*. Master's thesis, Zhejiang University, Hangzhou in China.

Zhang, Q., Mills, J.K., Cleghorn, W.L., Jin, J., and Sun, Z. (2015). Dynamic model and input shaping control of a flexible link parallel manipulator considering the exact boundary conditions. *Robotica*, 33(6), 1201–1230.